System Scheduling with Pumped-Hydro Plants with Different Grid Connection Schemes

System Scheduling with Pumped-Hydro Plants with Different Grid Connection Schemes

Giordano Costanzi, Vincenzo Trovato
Department of Civil, Environmental, Mechanical Engineering
Università di Trento
Trento, Italy
giordano.costanzi@unitn.it
vincenzo.trovato@unitn.it

Pietro Colella, Gianfranco Chicco
Department of Energy "Galileo Ferraris"
Politecnico di Torino
Torino, Italy
pietro.colella@polito.it
gianfranco.chicco@polito.it

***Abstract*—The increase in inverter-connected generation sources is causing a remarkable decline in the overall system inertial response, which shall be balanced by a significant amount of frequency response services. This represents a significant challenge against the ability to ensure secure and reliable power networks whilst implementing a cost-effective transition towards a low carbon paradigm. This paper assesses the value of providing different types of flexible ancillary services from pumped hydro plants depending on their specific grid connections implementations. The flexibility envelopes associated to each implementation are included in a security-constrained system scheduling model. Case studies consider a low carbon system scenario of the Great Britain and highlight the value of providing both inertial and frequency responses.**

Keywords—security constrained system scheduling, flexibility, pumped hydro storage, inertial response, frequency response

I. INTRODUCTION

The decline in Natural Inertia (NI) [1] as consequence of the integration of large shares of inverter-connected Renewable Energy Sources (RES) sets significant challenges to the secure and cost-effective operation of future low-carbon power networks. In the aftermath of a sudden large generation outage, the network frequency and its rate of change may reach intolerable values unless significant amounts of ancillary services are rapidly delivered. In this context, there is a growing interest in the flexibility granted by Pumped Hydro Storage Plants (PHSPs). In some countries, the installed capacity of hydro-generation has not saturated yet the potential capacity of available water reservoirs [2], paving the way to new projects. In other areas, where the exploitation of new reservoirs is limited [3], traditional impoundment facilities are being upgraded to PHSPs. In both cases, this positively helps the fulfilment of system-level requirements of NI and Primary Response (PR), i.e. ancillary services characterized by a rapid delivery. Note that the ability to provide NI and PR ultimately depends on the grid-connection scheme of each PHSP. The schemes considered in this work envisage one reversible pump/turbine machine or two separate hydraulic units coupled to a synchronous generator, directly connected to the grid, or an asynchronous unit, connected to the grid by means of power electronics.

Overall, the techno-economic impact stemming from the flexible operation of PHSPs has been studied in the literature. For instance, PHSPs have been incorporated into a unit-commitment formulation with inertia-dependent constraints [4]. However, the PHSP formulation does not account for various types of grid connection. A similar approach is reported in [5]; although different configurations of PHSPs are considered, the study does not well incorporate the NI and PR requirements, limiting the added value from PHSPs.

This work has been developed as part of the OASIS 4 ENERGY project, funded by the European Union - NextGenerationEU PRIN 2022 PNRR Prot. n. P2022MLE3L, CUP-E53D23014720001, Mission 4 "Education and Research" - Component C2 - Investment 1.1.

The same features characterize the methodologies in [6], [7]. A price-taker approach in [8] assessed the optimal operation of a single PHSP to deliver multiple services in response to different price signals. A stochastic medium-term scheduling problem dispatches a PHSP in [9] whilst accounting for environmental constraints on the water reservoirs.

This work contributes to the existing literature by proposing a detailed system Security-Constrained System Scheduling (SCSS) model that minimizes system operation costs whilst accurately computing system-level requirements for NI, PR, Secondary Response (SR) and spinning and standing reserves. Four grid-connection schemes for PHSPs are considered, i.e., Fixed Speed Synchronous Motor (FSSM), variable-speed units such as Doubly Fed Induction Motor (DFIM) and Full Converter Synchronous Motor (FCSM), and Ternary Turbine Synchronous Motor (TTSM) operated by means of the hydraulic short circuit. Depending on the actual features of each grid connection scheme, PHSPs may be able to contribute to all or only some of the ancillary services above. Moreover, the techno-economic impact of PHSPs is computed considering the presence of other flexible assets such as, aggregate Thermostatically Controlled Loads (TCLs) and High-Voltage Direct-Current (HVDC) links. The methodology is applied to a future low-carbon system scenario of the Great Britain (GB) power system. Results indicate that a TTSM connection scheme provides the lowest annual system operational cost and RES curtailment index. This is due to the twofold ability for a PHSP under this configuration to supply NI and regulate the power output to provide other services (e.g., arbitrage, PR, SR and reserves).

II. GRID CONNECTION SCHEMS FOR PHSPS

The choice of a grid connection scheme for PHSPs is not straightforward and may depend on several factors. Lately, the decision may also be affected by the growing system-level demand in ancillary services, specifically NI and PR. In fact, the particular type of grid connection may grant or (partially) impede the provision of NI and PR from a PHSP. Four grid connection schemes are considered in this paper and the corresponding features are listed below:

- *Fixed Speed Synchronous Motor (FSSM)*: a reversible (pump/turbine) hydraulic machine is connected to a synchronous unit and thus to the grid, contributing to the NI; Power regulation is allowed in turbine mode, although limited to a certain range, whereas it is impeded in pump mode, letting the plant absorb power up to the rated capacity only [10].
- *Doubly Fed Induction Motor (DFIM)*: the hydraulic unit is reversible and connected to an asynchronous generator/motor. The setup is interfaced with the grid via converter, which allows limited power regulation both in pump and turbine mode. Nonetheless, the presence of the converter prevents the PHSP from providing NI [11]. In this case, note that the size of the converter is typically

lower than the size of the plant (e.g., 15-30% of the rated capacity [12]).

- *Full Converter Synchronous Motor (FCSM)*: the same overall features are offered by the FCSM. Although a synchronous machine is adopted, the provision of NI is impeded by the presence of the converter. The latter has the same rated capacity of the plant.
- *Ternary Turbine Synchronous Motor (TTSM)*: two distinct hydraulic machines, a pump and a turbine, are connected to the same shaft of a synchronous unit. The setup is operated by means of the hydraulic short circuit. The additional complexity allows power regulation both in pump and turbine modes whilst contributing to NI [13].

Further details on the actual power regulation ranges for the four schemes are shown in Fig. 1. Black and grey areas indicate attainable operating levels in turbine and pump mode, respectively. Note that the pump under the TTSM scheme can also operate at maximum rated capacity.

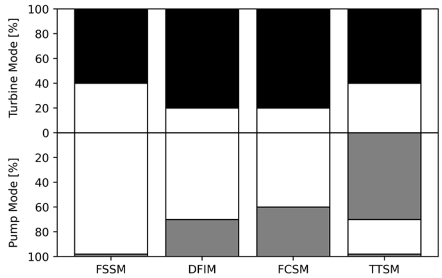

Fig. 1 Power regulation capabilities under the grid connection schemes considered. Black/grey areas refer to turbine/pump mode, respectively.

The flexibility granted by the power regulation ranges can be exploited in regular operation to better assist net-load variations. Similarly, such flexibility can be employed to provide frequency response (e.g., PR and SR) and reserve (spinning R_{sp} or standing R_{st}) services. The short delivery time of PR (5-10 s) limits the actual power headroom to deliver the service. The numerical values adopted in this paper are reported in Table I and are expressed as percentage of the rated capacity. Considering the FSSM, the headroom for PR is nil in pump model in accordance with Fig. 1; in turbine mode, the relatively small value (5%) reflects the transient droop compensation required by governors of FSSM hydraulic units for stable speed control performance [14].

TABLE I PRIMARY RESPONSE HEADROOM [% OF THE RATED CAPACITY]

mode	**grid connection scheme**			
	FSSM	***DFIM***	***FCSM***	***TTSM***
pump	0%	20%	20%	10%
turbine	5%	20%	20%	10%

The values of the headroom for the DFIM and FCSM increase (20%) due to the fast response capabilities of the converter [15]. The lack of power electronics in the TTSM case is responsible for lower headroom (10%), although this is higher than in the FSSM scheme. The longer delivery times for SR and reserve services allow the PHSPs to make full use of the entire power regulation ranges in Fig. 1 to provide these services. The mathematical formulation of the constraints on the PHSP operation is shown in Section III-B.

III. MODEL DESCRIPTION

The benefits from the flexible operation of a PHSP under the grid connection schemes indicated in Section II are evaluated by means of the proposed SCSS model. The schematics of the underlying GB power system model are illustrated in Fig. 2. The GB system is interconnected to Norway, Germany and France via HVDC links. These are employed for inter-area energy-exchange only; their operation depends on the energy prices in the connected areas. Synchronous generators are also modelled, including nuclear plants, thermal plants (with Open-Cycle Gas Turbines – OCGT, and Combined Cycle Gas Turbines – CCGT). RES consist of aggregate wind farms, photovoltaic (PV) farms, and Run-of-River (RoR) synchronous hydro plants. A single large PHSP is considered with the possibility to connect it to the grid under the connection schemes in Section II. Other assets are smartly controlled TCLs [16].

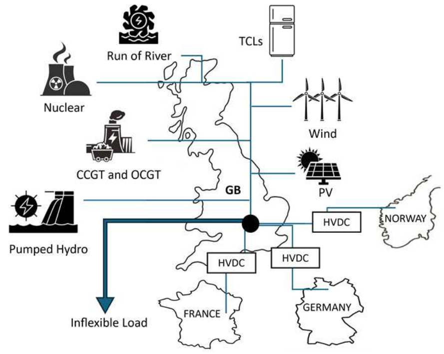

Fig. 2 Schematics of the interconnected system.

The list of ancillary services considered is shown in Table II, together with the characteristics and list of providers.

TABLE II CHARACTERISTICS OF THE ANCILLARY SERVICE

Type	***Characteristic***	***Providers***
NI	*Kinetic energy stored in the rotating masses of synchronous units. Focus on RoCoF and nadir conditions.*	Synchronous generators, RoR, FSSM, TTSM
PR	*Automatic power change supplied by 10s. Focus on RoCoF and nadir.*	Thermal, TCLs, PHSP
SR	*Automatic power change supplied by 30s and sustained for tens of minutes. Focus on quasi-steady state condition.*	Thermal, TCLs, PHSP
R_{sp}	*Long term power change to restore the steady state. Providers are already on*	Thermal, PHSP
R_{st}	*Long term power change to restore the steady state. Providers are not online.*	OCGT, PHSP

Notably, nuclear power plants do not provide frequency response services besides NI. In contrast, thermal generators provide full access to the range of ancillary services. Additionally, the actual delivery of more energy intensive services such as SR requires TCLs to perform an energy recovery pattern to be completed by the same scheduling interval as in [16]. This ensures the feasibility of providing ancillary services in the subsequent timestep.

A. The Security Constrained System Scheduling model

The proposed deterministic SCSS minimizes the annual system operational cost defined in (1a) as the sum of the generation costs φ_i (1b), the HVDC cost for power import/export χ_i (1c), the RES curtailment costs ψ_i (1d) and the cost for spinning and standing reserves Ω_i (1e). The extended mathematical model is reported in [16].

$$min \sum_{i=1}^{2T} (\varphi_i + \chi_i + \psi_i + \Omega_i) \tag{1a}$$

$$\varphi_i = \varphi_i\left(P_{g,i}, N_{g,i}^{up}, N_{g,i}^{su}\right) \tag{1b}$$

$$\chi_i = \chi_i\left(P_{l,i}^{im}, P_{l,i}^{ex}\right) \quad (1c) \qquad \psi_i = \psi_i\left(P_{\gamma,i}^{cu}\right) \quad (1d)$$

$$\Omega_i = \Omega_i\left(N_{g,i}^{sta}, N_{g,i}^{spin}\right) \tag{1e}$$

Note that, φ_i refers to all the conventional units $g \in \mathcal{G}$, it depends on the dispatch output $P_{g,i}$, the number of units online $N_{g,i}^{up}$ and the number of those that are starting up $N_{g,i}^{su}$. Considering the HVDC link $l \in L$, the variables $P_{l,i}^{im}$ and $P_{l,i}^{ex}$

represent the importing (to the GB) and exporting (from the GB) power through the interconnectors, respectively. Moreover, RES curtailment is expressed by $P_{\gamma,i}^{cu}$ for all the sources $\gamma \in \Gamma$. Finally, Ω_i accounts for expected delivery cost to provide reserves; it does depend on the number of conventional units providing standing reserve $N_{g,i}^{st}$ in accordance with the limitations in Fig. 1, the amount of committed spinning and standing reserves from thermal units $R_{g,i}^{sp}$ $R_{g,i}^{st}$ and from the PHSP, i.e. R_i^{sp} R_i^{st}. The horizon of the analysis is one year, with 365 individual simulations. The time interval of each simulation is $2T$=96 steps, i.e., 48 h. The solution beyond the first day is discarded. When moving to the next roll, relevant inter-temporal constraints are maintained. The main constraints are:

$$\sum_{g\in\mathcal{G}} P_{g,i} + P_i^d - P_i^c + \sum_{l\in I}\{P_{l,i}^{im} - P_{l,i}^{ex}\} + \sum_{\gamma\in\Gamma}\{P_{\gamma,i} - P_{\gamma,i}^{cu}\} = L_i \tag{2}$$

$$H_i\,\Theta_i \geq q_i^* \tag{3}$$

$$\Theta_i\, t_\rho^2 - 2\,\Delta P_L\, t_\rho\, t_\theta - 4\,\Delta f_\rho\, t_\theta\, H_i \geq 0 \tag{4}$$

The equality constraint (2) represents the load balance equation, where P_i^d and P_i^c are the power output of the PHSP in turbine and pump mode, respectively. $P_{\gamma,i}$ is the available RES generation and L_i is the system level load. Furthermore, (3)-(4) ensure, respectively, enough allocation of NI and PR to maintain the frequency nadir and RoCoF above the corresponding minimum thresholds. In particular, the derivation of (3) is in [16], which highlights that the numerical value of q_i^* depends on the system load at step i and the maximum infeed generation loss ΔP_L. The left-hand side represents the product between the committed NI (H_i) and PR (Θ_i). The expressions of these quantities are in (5)-(6), respectively. Note that f_0 is the nominal system frequency (50 Hz); H_g and $\overline{P}_g$ are the constant of inertia and rated capacity of a single conventional plant of technology g. Moreover, ζ_i represents the contribution to NI from the PHSP; more details are provided below, depending on the particular grid connection scheme. H_γ and $\overline{P}_\gamma$ are the constant of inertia and rated capacity of RES technologies. In this work, only RoR synchronous units have a non-zero H_r. Wind and PV plants do not provide any ancillary service. Finally, H_L is the constant of inertia associated to the maximum infeed loss ΔP_L.

$$H_i = \sum_{g\in\mathcal{G}} \frac{H_g\,\overline{P}_g\,N_{g,i}^{up}}{f_0} + \frac{\zeta_i}{f_0} + \sum_{\gamma\in\Gamma}\frac{H_\gamma \overline{P}_\gamma}{f_0} - \frac{H_L \Delta P_L}{f_0} \tag{5}$$

$$\Theta_i = \Theta_i^c + \Theta_i^d + \sum_{g\in\mathcal{G}} \Theta_{g,i} + \Theta_i^{TCL} \tag{6}$$

In (6), Θ_i^c and Θ_i^d are the PR contribution from the PHSP in pump and turbine mode, respectively. $\Theta_{g,i}$ accounts for the PR support from synchronous units to which RoR units are assumed to not participate; in fact, small machines may not be equipped with governors. Θ_i^{TCL} is the support from TCLs. Finally, t_ρ (0.5 s) in (4) is the measuring time for RoCoF settings, t_θ (10 s) is the delivery time for PR, and Δf_ρ (0.5 Hz) is the maximum frequency deviation for RoCoF purposes.

The objective function (1a) is subject to other typical constraints of SCSS models as in [16]. Constraints on synchronous generators impose the feasibility of the dispatch level and the committed ancillary services, the respect of intertemporal constraints (min up and down, ramping, etc.). Constraints on TCLs impose sufficient power and energy limits to the regular operation and to the provision of PR and SR, including the energy recovery pattern. Other constraints refer to the HVDC operation; at each time step i the power is limited to the rated capacity and the flow may occur in one direction only. Finally, other system-level constraints allocate enough SR, R_{sp} and/or R_{st} to restore a nominal condition pursuant to the infeed generation loss ΔP_L.

B. Modelling the flexible operation of PHSPs

Constraints on the flexible operation of the PHSP integrated in the SCSS model are provided in this section. Note that (7)-(16) can be applied to all the grid-connection schemes in Section II without major changes. Other constraints may require ad-hoc formulation, which is provided below for each connection scheme, as needed.

$$S_{i+1} = S_i + \left(\eta\, P_i^c - P_i^d/\eta\right)\Delta t \tag{7}$$

$$\underline{S} \leq S_i \leq \overline{S} \tag{8}$$

$$0 \leq \Theta_i^d \leq h_\theta^d\, u_i^d\, \overline{P} \tag{9}$$

$$0 \leq \Theta_i^c \leq h_\theta^c\, u_i^c\, \overline{P} \tag{10}$$

$$u_i^d\, \underline{P}^d \leq P_i^d \leq u_i^d\, \overline{P} \tag{11}$$

$$\Theta_i^d \leq \overline{P} - P_i^d \quad (12) \qquad 0 \leq \sigma_i^d \leq \overline{P} - P_i^d \tag{13}$$

$$S_i - t_\sigma\left(P_i^d + \sigma_i^d\right)/\eta \geq \underline{S} \tag{14}$$

$$R_i^{sp} \leq \overline{P} - P_i^d - max\{\Theta_i^d, \sigma_i^d\} \tag{15}$$

$$S_i - t_{\mathcal{R}}\left(P_i^d + R_i^{sp} + R_i^{st}\right)/\eta \geq \underline{S} \tag{16}$$

Constraints (7)-(8) limit the energy evolution S_i also depending on the selected mode (turbine or pump); note that η is a unitless efficiency. Constraints (9)-(10) limit the provision of PR in turbine and pump mode, respectively. The values of the headroom h_θ^d and h_θ^c are indicated in Table I, highlighting that the FSSM scheme does not allow the provision of PR in pump mode. Note that u_i^d and u_i^c are binary variables which enable the turbine or pump mode, respectively; more details on the relationship between these variables are provided later. $\overline{P}$ is the rated capacity of the PHSP. Furthermore, (11) sets the power regulation range in turbine mode, envisaged for all the grid connection schemes up to different extent. As in Fig. 1, the minimum stable level $\underline{P}^d$ is equal to $0.4\,\overline{P}$ for the schemes FSSM and TTSM, and to $0.2\,\overline{P}$ for the DFIM and FCSM. The allocated PR in turbine mode is linked in (12) to the dispatch level. Constraint (13) is similar to (12) and applies to the allocated SR in turbine mode, σ_i^d. The objective of (14) is to maintain the energy level pursuant to the provision of σ_i^d in excess to P_i^d and for a time t_σ (10 min) above the minimum threshold. The commitment time for PR is much smaller than t_σ, avoiding the need for a constraint on PR similar to (14). The power headroom for spinning reserve R_i^{sp} is in (15), whereas a safe energy level after the deployment of spinning or standing reserve is ensured by (16). Here, $t_{\mathcal{R}}$ is the commitment time for reserves (4 h). As formulated later, the PSHP cannot provide both reserves, simultaneously. Hence, (16) applies to $P_i^d + R_i^{sp}$ or R_i^{st}.

Constraints (17)-(33) depend on the grid connection scheme. With respect to the FSSM scheme, (17)-(20) apply:

$$u_i^d + u_i^c \leq 1 \quad (17) \qquad P_i^c = u_i^c\,\overline{P} \tag{18}$$

$$\left[1 - \left(u_i^d + u_i^c\right)\right]\underline{P}^d \leq R_i^{st} \leq \left[1 - \left(u_i^d + u_i^c\right)\right]\overline{P} \tag{19}$$

$$\zeta_i = \left(u_i^c + u_i^d\right) H\,\overline{P} \tag{20}$$

In general, a PSHP cannot operate in pump and turbine mode simultaneously. This is ensured by (17), which also enables the idle condition. The inability of power regulation for the FSSM in pump mode (see Fig. 1) is expressed in (18); if in pump mode, the FSSM scheme only allows to operate the pump at the rated capacity. As explained before, standing reserve R_i^{st} can be allocated only if the PHSP is idling; if so, any level between $\underline{P}^d$ and $\overline{P}$ can be chosen (19). The expression ζ_i (20) represents the contribution to the NI from synchronous FSSM units. The contribution is enabled both in pump and in turbine mode; in this case H=4 s.

Constraints (21)-(25) apply to DFIM and FCSM schemes:

$$u_i^d + u_i^c \leq 1 \quad (21)$$

$$\left[1-\left(u_i^d+u_i^c\right)\right] \underline{P}^d \leq R_i^{st} \leq \left[1-\left(u_i^d+u_i^c\right)\right] \overline{P} \quad (22)$$

$$u_i^c\, \underline{P}^c \leq P_i^c \leq u_i^c\, \overline{P} \quad (23)$$

$$\Theta_i^c \leq P_i^c - \underline{P}^c \quad (24) \qquad 0 \leq \sigma_i^c \leq P_i^c - \underline{P}^c \quad (25)$$

Constraints (21) and (22) have the same objective of (17), and (19), respectively. The converter-interface schemes envisage power regulation in pump mode (23) with $\underline{P}^c$ equal to $0.7\,\overline{P}$ (DFIM) and $0.6\,\overline{P}$ (FCSM) – see Fig. 1. Such capability in pump mode opens up to the allocation of PR (24) and SR (25), respectively. However, DFIM and FCSM do not contribute to the NI, always letting ζ_i being equal to zero.

Finally, concerning the TTSM scheme, (26)-(33) apply:

$$u_i^d + u_i^c + z_i^c \leq 1 \quad (26)$$

$$u_i^c\, \underline{P}^c \leq \tilde{P}_i^c \leq u_i^c\, \tilde{P} \quad (27)$$

$$\hat{P}_i^c = z_i^c\, \overline{P} \quad (28) \qquad P_i^c = \hat{P}_i^c + \tilde{P}_i^c \quad (29)$$

$$\Theta_i^c \leq \tilde{P}_i^c - \underline{P}^c \quad (30) \qquad 0 \leq \sigma_i^c \leq \tilde{P}_i^c - \underline{P}^c \quad (31)$$

$$\left[1-\left(u_i^d+u_i^c+z_i^c\right)\right] \underline{P}^d \leq R_i^{st} \leq \left[1-\left(u_i^d+u_i^c+z_i^c\right)\right] \overline{P} \quad (32)$$

$$\zeta_i = \left(u_i^c + u_i^d + z_i^c\right) H\, \overline{P} \quad (33)$$

The operation of a PHSP, obtained by means of the hydraulic short circuit, requires an additional binary variable z_i^c in pump mode (26). On the one hand, u_i^c refers to the operation in pump mode within the power regulation range (27), i.e. $[\underline{P}^c, \tilde{P}]$ with $\underline{P}^c$=0 and $\tilde{P} = 0.7\,\overline{P}$ (see Fig. 1). On the other hand, z_i^c tracks the pump operation $\hat{P}_i^c$ of the PSHP when it absorbs the rated capacity (28). As in Fig. 1, the unit under the TTSM scheme cannot operate in the interval $\left]\tilde{P}, \overline{P}\right[$. Constraint (29) clarifies the actual pump operation to be used in (7) and (2). The aim and structure of (24)-(25) is extended to (30)-(31), requiring the use of the flexible power level $\tilde{P}_i^c$. Similarly, (32) extends (22) with the addition of z_i^c to identify the idle operation. Last, the contribution to the NI is offered by (33); Since the TTSM envisages a ternary setup with a different pump and a turbine, in addition to the synchronous generator, the related constant of inertia H is higher (6 s).

IV. Case Study and Results

Simulations are carried out considering typical future energy scenario of the GB interconnected system in Fig 2. Reference values and half-hourly input data are mainly from [16]. Minimum and maximum values for L_i are 22 GW and 56 GW, respectively; the total annual energy demand is 655 TWh. Six nuclear power plants of rated capacity 1800 MW are considered. The OCGT fleet consists of 25 units of 200 MW, whereas the CCGT generation is made of 90 units of 500 MW. The production costs for nuclear, OCGT and CCGT are 10 £/MWh, 101 £/MWh and 51 £/MWh, respectively. Concerning RES, the installed capacities of wind, solar and RoR generation are 70 GW, 30 GW and 5 MW, respectively. Collectively, the potential annual RES generation reaches 484 TWh. The curtailment cost for wind generation is 80 £/MWh; similarly, the same type of cost is 70 £/MWh for PV generation and 90 £/MWh for RoR plants. The aggregate steady state power consumption of TCLs is 2.5 GW. The rated capacity of the GB-France HVDC link is 2 GW, whereas the other two links have a single rated capacity equal to 1.4 GW. The HVDC import/export prices are taken from [17].

A single large PHSP is modelled with rated capacity 2.5 GW and with $\overline{S}$=20 GWh and $\underline{S}$=0 GWh. The same efficiency η applies in pump and turbine mode; numerical values are 0.85 (FSSM), 0.86 (DFIM and TTSM) and 0.87 (FCSM), as detailed in [12]. Four main simulations are carried out; each of them envisages the PHSP connected to grid with one of the schemes reported in Section II. The reference case refers to the FSSM scheme. Each scenario is assessed considering two sets of HVDC prices. The reference choice adopts the 2019 data (low average values and minor variability); the latter uses the 2022 data (high average values and major variability). Simulations are carried out using the Julia programming language and Gurobi solver with a MIPGap of 1% on a 16 GB RAM IntelCore i7 machine. Average simulation time is 483 s.

A. System-level impact of connection schemes for PHSPs

The annual system operational cost for the base case (FSSM) is equal to 11.61 b£, with a total RES curtailment of 21.54%. Percent reductions obtained under the other scenarios and with respect to the base case are reported in Fig. 3. Scenarios with variable speed setups, i.e., DFIM and FCSM, lead to a reduction in both operational cost (3.51% and 3.53%, respectively) and in RES curtailment (4.04% and 4.16%, respectively). These results stem from the wider ranges for power regulation granted by the DFIM and FCSM schemes. The benefits concerning the power regulation, to be also employed to provide thus PR and SR, overcome the drawback of not being able to provide NI under these setups. The ability to offer both power regulation and NI support for a PHSP under the TTSM lets the largest reduction in system operational cost (4.63%) and RES curtailment (4.97%).

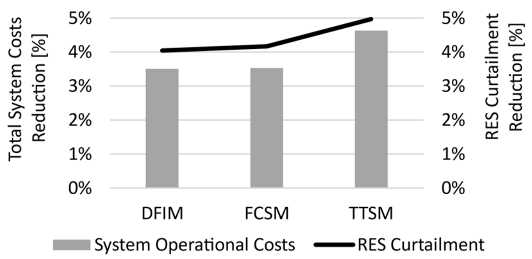

Fig. 3 Percent reduction in annual system operational cost (bars) and RES curtailment index (line) with respect to the Base Case – FSSM.

Similar trends are obtained when the half-hourly energy prices relevant to the three HVDC links refer to 2022. The larger amplitude and variability of prices exhibited in 2022 lead to more significant reduction in system operational cost. The annual system cost and RES curtailment index under the base case (FSSM) are 4.05 b£ and 22.46%, respectively. Percent reductions considering the other three grid connection schemes for PHSPs are reported in Table III.

TABLE III Variation Compared to FSSM with 2022 HVDC Prices [%]

	DFIM	FCSM	TTSM
Sytem operational cost	-9.70%	-9.72%	-12.43%
RES curtailment	-4.00%	-4.07%	-4.87%

The results in Fig. 3 can be explained by assessing the median allocation of NI and PR at each half-hour of the year (top and bottom of Fig. 4). The ability to maintain the post-fault frequency nadir above a minimum threshold depends on the procurement of enough NI and PR. A lower availability in NI would require larger amounts of PR and vice versa. It is evident that connection schemes which maintain PHSPs synchronous with the system frequency, i.e., FSSM (solid black) and TTSM (dashed grey), allow for higher allocation of NI compared to the DFIM (solid grey) and FCSM (dashed black). In parallel, the system allocation of PR is lower with FSSM and TTSM compared to the DFIM and FCSM.

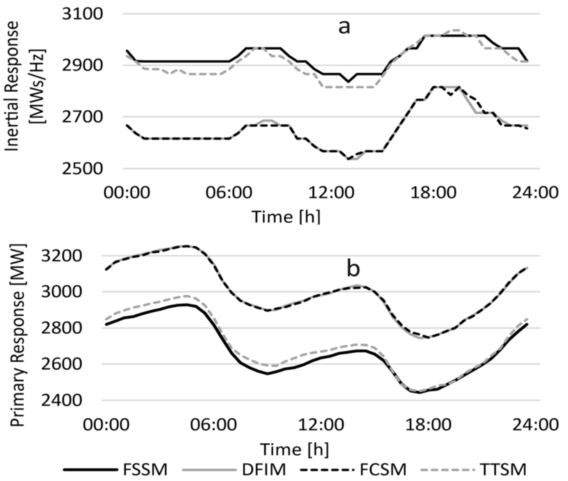

Fig. 4 Median half-hourly inertial response (a) and primary response (b).

It is worth noting that the amount of NI needed under the TTSM case is slightly lower than under the FSSM case, whereas opposite trends are reported concerning the PR allocation. This result has a twofold motivation and it is responsible of the economic benefits in Fig. 3. First, PHSPs with a ternary scheme have a larger constant of inertia compared to the FSSM case (since two hydraulic machines have a higher momentum of inertia rather than a single reversible one). Second, TTSM plants can provide power regulation and thus PR also in pump mode operation (this is not doable with FSSM plants). Especially in presence of high-RES/low-demand conditions, being able to provide more NI and more PR with the same PHSP is crucial. Ultimately TTSM avoids the commitment of some cost-intensive thermal generators (significant marginal and start-up costs). Results in Fig. 5 indicate lower average value of online thermal units (excluding nuclear) under the TTSM (dashed grey) compared to the FSSM (solid black). Finally, the milder reductions in system operational costs with the DFIM and FCSM are due to their inability to provide NI, which is only partially balanced by a higher range for power regulation and headroom for PR. These features ensure a minor reduction in the number of committed thermal units.

B. *Operation of PHSPs with different connection schemes*

This section focuses on the operation of the PHSP under the different configurations. Fig. 6 shows the median (over the year) half-hourly power levels in pump mode. Note that the assessment of the median pump consumption excludes those time intervals when the PSHP is in turbine mode or idling.

The most preferred operation under the FSSM, DFIM and FCSM is the maximum power consumption. For the FSSM, this is the only option since no power regulation is possible in pump mode (Fig. 1).

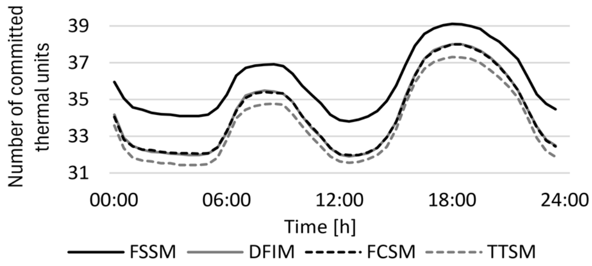

Fig. 5 Average half-hourly number of committed thermal generators.

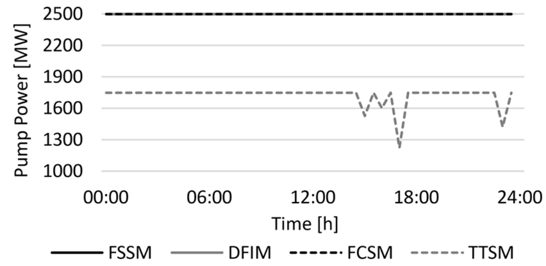

Fig. 6 Median half-hourly pump power level with different PHSP schemes.

The two converter-based schemes operate at high power levels to contribute to the RES integration and, at the same time, fully employ the headroom for PR (Table I). On the other hand, the TTSM favors a lower consumption in pump mode. As illustrated in Fig. 1, operating at 70% of the rated capacity (i.e., 1750 MW) allows to still integrate available RES whilst being able to modulate the consumption for PR and to contribute to NI. The PR provision would be impeded if the PHSP operates at the maximum consumption due to the restrictions of the TTSM (Fig. 1).

A similar assessment deals with the median power levels in turbine mode. Results are shown in Fig. 7 and indicate almost the same median operation for DFIM and FCSM. A different approach regards the FSSM and TTSM cases.

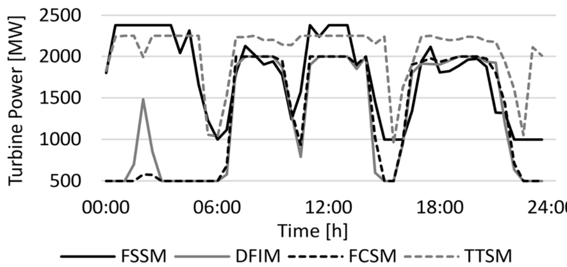

Fig. 7 Median half-hourly turbine power level with different PHSP schemes.

The turbine output of the converter-interfaced PHSP is lower than the one of synchronous PHSP. This is more evident during the time interval 00:00-06:00. It must be noted that any PHSP would operate in turbine mode during those hours if the RES availability is not remarkably high. If that is the case, the synchronous PHSP operates relatively close to maximum capacity to feed the load, leveraging on its low production cost. At the same time, it provides both NI and the entire PR headroom (higher in the TTSM case). DFIM and FCSM turbines operate at lower power output, although they can still provide the maximum PR headroom. However, since converter-interfaced PHSPs do not contribute to NI, the system needs conventional generators to cover for this lack. If thermal units are committed, they shall respect minimum generation level, forcing the PHSP to operate part-loaded.

The interplays stemming from results in Fig. 6-7 are validated by Fig. 8. Focusing on turbine mode, it is clear how the NI contribution of synchronous PHSPs, especially if in combination with the PR provision (TTSM), allows to shutdown more thermal generators compared to asynchronous PHSPs. In fact, in this case the FSSM performance is equivalent to the one of more flexible DFIM and FCSM. Conversely, in pump mode, the operation of synchronous units is affected by the lack of power regulation of FSSM and reduced range for regulation (only enabled if the operating point is below 70% of the rated capacity) for the TTSM. Hence, in this case, the FSSM requires a larger number of thermal units online compared to the other cases. Moreover, the typically higher benefits of the TTSM, with respect to asynchronous schemes, are not evident in this case.

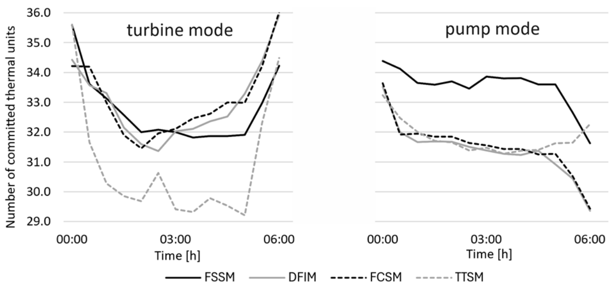

Fig. 8 Average number of committed thermal units for the time interval 00:00 – 06:00 in turbine mode (left) and pump mode (right).

Finally, the analysis of the operation of the PHSPs under different grid connection schemes requires the assessment of the utilization factors in Fig 9, i.e., the total number of hours spent in pump or turbine mode with respect to the total number of hours in the year. Overall, the FSSM scheme exhibits lower utilization with respect to the other schemes. Synchronous PHSPs (FSSM and TTSM) can operate more often in pump mode since they can still provide NI (and PR with the TTSM) and increase the consumption to integrate more RES and cause less high-cost curtailments. Nonetheless, the inability of converter-interfaced schemes to provide NI is compensated by the ability to regulate power also in pump mode, letting the relevant utilization factors quite close to the one. A more remarkable difference remains with respect to the TTSM since the latter can both provide NI and PR via power regulation in pump mode. Opposite results refer to the turbine mode. The TTSM reduces the time spent in turbine mode to give more space to the integration of RES.

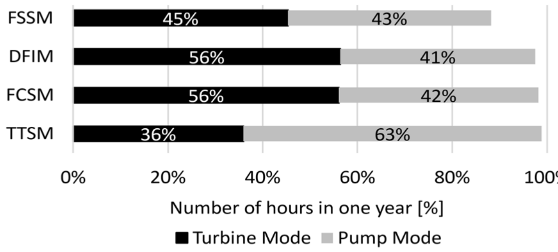

Fig. 9 Annual utilization factor for turbine and pump operations.

V. Conclusion

This work assessed the impact of PHSPs with different grid connection schemes on the security and economics of future low-carbon power systems. A novel SCSS model aims to minimize the system operational costs whilst allocating a variety of ancillary services to ensure secure post-fault frequency dynamics. A dedicated set of MILP constraints has been developed to acknowledge the different level of flexibility granted by these configurations. Results have highlighted the techno-economic benefits provided by PHSPs under the TTSM scheme. In fact, system operations and security benefit from the twofold support, i.e. provision of NI and power regulation, both in pump and turbine mode, granted by the TTSM scheme. The ability to rapidly regulate the power level allows this configuration to provide PR. None of the other PHSP configurations are able to provide the similar level of flexibility. Besides system-level metrics, the proposed analysis has investigated the typical operation requested by the single PHSP under the different configurations.

Future work will implement further intertemporal constraints on the operation of a PHSP including the ability to rapidly switch operational regimes and model the variations to the energy level of the PHSP due to actual water inflows.

Acknowledgment

Views and opinions expressed are those of the authors only and do not necessarily reflect those of the European Union or European Commission. Neither the European Union nor the granting authority can be held responsible for them.

References

[1] L. Yan *et al.*, “Study on Requirement of Control and Stability with Renewable Energy Generation Grid Integration,” *APAP 2019 - 8th IEEE International Conference on Advanced Power System Automation and Protection*, 2019.

[2] M. Bilgili, H. Bilirgen, A. Ozbek, F. Ekinci, and T. Demirdelen, “The role of hydropower installations for sustainable energy development in Turkey and the world,” *Renew. Energy*, vol. 126, pp. 755-764, 2018.

[3] M. Gimeno Gutierrez and R. Lacal Arantegui, “Assessment of the European potential for pumped hydropower energy storage: A GIS - based assessment of pumped hydropower storage potential,” Publications Office of the European Union, Luxembourg, 2013.

[4] V. Trovato, A. Bialecki, and A. Dallagi, “Unit Commitment with Inertia-Dependent and Multispeed Allocation of Frequency Response Services,” *IEEE Trans. Pow. Syst.*, vol. 34, no. 2, 1537–1548, 2019.

[5] O. Alizadeh-Mousavi and M. Nick, “Stochastic Security Constrained Unit Commitment with variable-speed pumped-storage Hydropower Plants,” *19th PSCC 2016*, 2016.

[6] H. Y. Su *et al.*, “Developing an Optimal Scheduling of Taiwan Power System with Highly Penetrated Renewable Energy Resources and Pumped Hydro Storages,” *IEEE Trans Ind Appl*, vol. 57, no. 3, pp. 1973–1986, 2021.

[7] Z. Zhang, X. Gao, L. Zhou, J. Liu, Y. Sun, and Y. Dong, “Joint Optimal Dispatching Strategy of Pumped Storage and Thermal Power Units with Large-Scale Wind Power Integration,” *5th IEEE Conference on Energy Internet and Energy System Integration: Energy Internet for Carbon Neutrality, EI2 2021*, 2021.

[8] X. Ma *et al.*, “Optimizing pumped storage hydropower for multiple grid services,” *J Energy Storage*, vol. 51, art. 104440, 2022.

[9] A. Alic, L. E. Schäffer, M. Toffolon, and V. Trovato, “Optimal price-based scheduling of a pumped-storage hydropower plant considering environmental constraints,” *Energy Systems*, 2023.

[10] E. Muljadi, R. M. Nelms, E. Chartan, R. Robichaud, L. George, and H. Obermeyer, “Electrical Systems of Pumped Storage Hydropower Plants: Electrical Generation, Machines, Power Electronics, and Power Systems,” United States, 2021.

[11] K. R. Vasudevan, V. K. Ramachandaramurthy, G. Venugopal, J. B. Ekanayake, and S. K. Tiong, “Variable speed pumped hydro storage: A review of converters, controls and energy management strategies,” *Renew. Sust. Energy Reviews*, vol. 135, art. 110156, 2021.

[12] H. Ye *et al.*, “Variable-speed Pumped Hydro Storage Technology: Overview, Solutions and Case Studies,” *2021 6th International Conference on Power and Renewable Energy, ICPRE 2021*, 2021.

[13] Z. Dong *et al.*, “Modeling and Simulation of Ternary Pumped Storage Hydropower for Power System Studies,” *IET Generation Transmission & Distribution*, vol. 13, no. 19, pp. 4382–4390, 2019.

[14] P. Kundur, *Power System Stability and Control*. 1994.

[15] W. J. Kim, Y. S. Lee, Y. H. Chun, and H. S. Jeong, “Reserve-Constrained Unit Commitment Considering Adjustable-Speed Pumped-Storage Hydropower and Its Economic Effect in Korean Power System,” *Energies (Basel)*, vol. 15, no. 7, 2022.

[16] V. Trovato, “Optimal coordination of spinning and standing reserve with energy payback of thermostatically controlled loads,” *Int. Journal of Electrical Power & Energy Systems*, vol. 149, art. 109041, 2023.

[17] “Ember Climate - European Wholesale Electricity Price Data.” [Online]. Available: https://ember-climate.org/data/data-tools/europe-power-prices/